Proceeding of the IEEE
International Conference on Robotics and Biomimetics
Dali, China, December 2019

Design of a Series Elastic Actuator with Double-layer Parallel Spring for Lower Limb Exoskeletons

Chaofeng Chen[1], Zhijiang Du[1], Long He[2], Linxiang Huang[1], Jiaqi Wang[1], Yongjun Shi[1], Guoqiang Xu[2], Fang Si[2], Tiantian Xiao[2], Dongmei Wu[1] and Wei Dong[1*]

1 State Key Laboratory of Robotics and System
Harbin Institute of Technology
Harbin, Heilongjiang Province, China

2 Weapon Equipment Research Institute
China South Industries Group Corporation
Beijing, China

***Abstract* – This paper presents a novel Series Elastic Actuator (SEA) with double-layer parallel spring for lower limb exoskeletons (LLE). The SEA can improve the human-robot interaction comfort and have the ability to absorb shock and vibration. In order to make the assembly process simple and convenient, the series elastic unit adopt split structure, which includes an inner ring structure, an outer ring structure and rectangular springs as elastic element. At the same time, in order to meet the requirements of the stiffness and dimensions of the SEA, a double-layer parallel spring arrangement is adopted. The stiffness of SEA is 312Nm/rad, which is obtained by the stiffness calibration experiment. In the experiments, the SEA is used in the knee joint of LLE and an impedance controller is designed to achieve knee joint tracking motion. Finally, the experiments results show the position tracking performance of the LLE, which illustrates the effectiveness of the SEA.**

Index Terms – Lower limb exoskeleton, Series Elastic Actuator, human-robot interaction, impedance control.

I. Introduction

The lower limb exoskeleton (LLE), as a research hotspot in the field of robotics, can play a significant role in enhancing human strength and assisting human rehabilitation [1-2]. The safety and comfort of the LLE is very important, as it is a typical human-robot interaction system. However, the traditional LLE uses rigid joints, does not have the ability to absorb shock, has poor safety and comfort, and cannot adapt to complex environments. In order to increase the comfort and safety of the LLE, the researchers proposed a series elastic structure between the motor and the load [3-5], namely the series elastic actuator (SEA). The structure has passive compliance, and the elastic element can generate a certain flexible deformation during the human-robot interaction process, which has a quality of absorbing shock and vibration. This increases the comfort and safety of the LLE and is suitable for working in complex environments. In addition, the joint torque can be feedback according to the deformation of the elastic element. The SEA can achieve precise force control and measure human-robot interaction for human intention estimation.

Now according to the type of elastic unit in SEA, it can be divided into two types, one is integral rotary elastic element and the other is linear springs. In the literature [6-8], several integral rotary elastic elements for SEA have been designed. Both of them consists of an inner ring, an outer ring and two sets of symmetrically distributed flexible beams. The flexible beams generate elastic deformation during the inner ring rotates relative to the outer ring, which can achieve passive compliance and slow down the impact. The design method of this type of elastic element is based on Finite Element Method (FEM) and optimized design. The elastic element in [6] has a lower stiffness, which requires the use of multiple elastic elements in parallel to increase stiffness and maximum torque. Besides, the actual stiffness of the elastic element in [7] is much smaller than the design stiffness, possibly due to the inconsistency between the actual material properties and the material properties in the simulation. In [8], the author proposed two elastic elements of the same structure and different sizes, one for measuring human-robot interaction and the other for measuring joint torque.

In the literature [9-11], there are several SEAs are designed, which based on the linear springs. Karavas et al. proposed a SEA based on the principle of leverage in [9]. One end of the lever is the input end and the other end pushes a pair of pre-compressed springs. The stiffness of the SEA can be changed by manually adjusting the position of the lever fulcrum. In [10], the author proposed a SEA for LLE knee joint. By moving the spring group up and down along the track, the SEA stiffness can be varied by changing the length of the force arm. In addition, a disc spring-based SEA for LLE is proposed in [11]. The experiments results show that the SEA with disc spring has high motion stability and can save energy. However, the disc spring has the disadvantage that the linearity is not very good, and the stiffness curves are inconsistent during loading and unloading.

According to the above analysis, two different types of SEA have their own advantages and disadvantages. The SEA with integral rotary elastic element is compact and easy to install. However, this elastic element is difficult to manufacture as a one-piece structure, and its deformation is mainly formed by bending at the flexible beam, which is relatively easy to fatigue damage. The SEA with linear spring is relatively easy to obtain the required stiffness and is easy to manufacture. However, this type of SEA may be relatively large in size. Through comprehensive consideration, a novel SEA with double-layer parallel spring is proposed to satisfy long-term stable use and have a small size.

* Corresponding author: Wei Dong (dongwei@hit.edu.cn)

978-1-7281-6321-5/19//$31.00 ©2019 IEEE

The main contribution of this paper is to design a novel SEA based on split structure and double parallel springs, which is easy to assemble and has small size and can be easily reconfigured to meet different stiffness requirements. In addition, an impedance control for the SEA in the LLE knee joint is presented to achieve position tracking. The experimental study demonstrates that the proposed control is superior in tracking performance.

The rest of this paper is organized as follows. In Section II, the design requirements and the double-layer parallel elastic unit will be described. In Section III, the design details of SEA will be introduced. In Section IV, the model and control strategy for the SEA are described. In section V, the preliminary experiments results are given. Conclusion and future work are given in Section VI.

II. Design Requirements And Double-Layer Parallel Elastic Unit

A. Design Requirements

The elastic unit is placed between the motor and the load to make the SEA passively compliant, so the stiffness selection of the elastic unit is important. If the stiffness is too large, it will be insensitive to torque changes, resulting in a decrease in control accuracy. If the stiffness is too small, the load action will be delayed. According to the conclusions of previous studies, the stiffness of elastic unit is generally chosen to be 100 to 300 Nm/rad [12], and the maximum torque range is 10 to 100 Nm [13]. According to the data in [14], more than 90% of the power spectral density of knee torque is in the frequency range of 0 to 4 Hz, so the minimum bandwidth of 4 Hz is set to the control requirement.

In order to make the LLE joint small in size and light in weight, the size of the elastic unit should also be in accordance with certain design requirements. That is, the thickness of the elastic unit should not exceed 30mm, and the diameter of the outer ring should be less than 100mm. Considering that the elastic unit needs to be mounted on a shaft with a diameter of 20 mm, the diameter of the inner ring is 20 mm. Besides, the inner and outer rings are connected to other parts by bolts. Table I gives a list of design requirements.

TABLE I
Design Requirements

Series spring stiffness	>200 Nm/rad
Peak torque	40 Nm
Torque bandwidth	>4 Hz
Output torque resolution	0.01 Nm
The thickness of the elastic unit	<30 mm
The diameter of the outer ring	<100 mm
The diameter of the inner ring	20 mm
Joint mass	<2.5 kg

B. Double-Layer Parallel Elastic Unit

According to the requirement of the SEA, a double-layer parallel elastic unit is designed, as shown in Fig. 1. To make the assembly process simple and convenient, the elastic unit the elastic unit adopts a split structure, including an outer ring structure, an inner ring structure and an elastic element. The outer ring structure consists of a triangular block, an outer ring of elastic, and a dowel pin. Triangular block and outer ring of elastic are fixed by screws. The dowel pin is connected to the triangular block through a threaded connection, the main function of which is to limit the radial displacement of the spring. The inner ring structure consists of ball pin and inter ring of elastic. The ball pin is connected to the triangular block through a threaded connection, so that the spring and the spherical surface can always maintain contact during the relative rotation of the inner and outer rings, which can ensure the stability of the motion process. The double-layered rectangular spring is used as the elastic element to meet not only small size requirements but also relatively large stiffness.

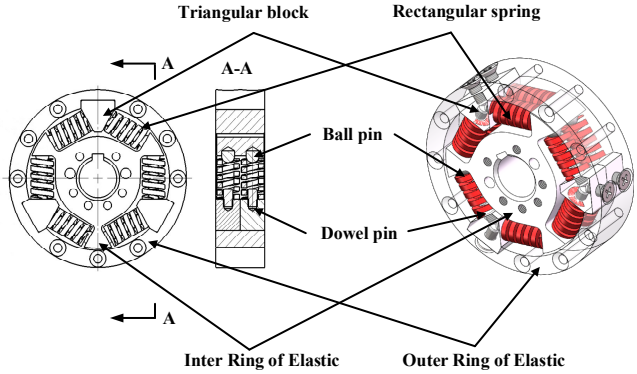

Fig. 1 Double-layer parallel elastic unit.

Since the rotation angle is very small, the motion of the spring is considered to be in a straight line, as shown in Fig.2. The stiffness of the spring can be obtained according to the following formula,

$$\begin{cases} N = \dfrac{T}{2n \times R} \\ \delta = R \times \tan \theta_m \\ K = \dfrac{N}{2\delta} \end{cases} \tag{1}$$

where N is the maximum force of the inner ring against the spring; T is the maximum torque experienced by the elastic unit; n is the number of spring groups; R is the distance from the center of the inner ring to the center of the spring; θ_m is the maximum angle of relative rotation between the inner and outer ring; δ is the maximum compression of the spring; K is the stiffness of the spring.

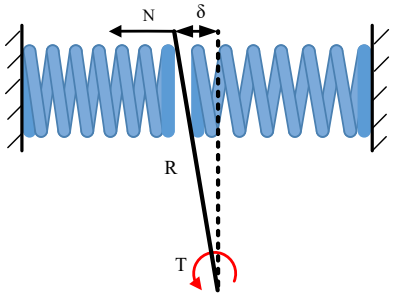

Fig. 2 The diagram of spring motion.

The final selected rectangular spring has an outer diameter of 12 mm, an inner diameter of 6 mm, an original length of 25 mm, a stiffness of 35.5 N/m and a stroke of 8 mm. The spring pre-compression is half of the stroke, i.e. 4mm. When one of the springs is fully compressed and the other parallel spring

returns to its original length, the compression force is maximized as shown below,

$$N = K \times 2\delta = 35.5 \times 2 \times 4 = 284\text{N} \quad (2)$$

Taking the distance from the center of the spring to the center of rotation is 29.5 mm, the maximum torque is expressed as follows,

$$T = N \times R \times 2n = 284 \times 0.0295 \times 2 \times 3 = 50.268\text{Nm} \quad (3)$$

The rotation angle can be expressed as follows,

$$\theta_m = \arctan\left(\frac{\delta}{R}\right) = \arctan\left(\frac{4}{29.5}\right) = 0.135\text{rad} \quad (4)$$

Therefore, the stiffness of the elastic unit is:

$$k = \frac{T}{\theta_m} = \frac{50.268}{0.135} = 372\text{Nm/rad} \quad (5)$$

It can be seen that the stiffness and maximum torque meet the design requirements.

In order to verify the strength of the inner ring of elastic, the finite element analysis was carried out. The material of the inner ring is aluminum alloy 6061, and its ultimate strength is about 124 MPa. Applying a torque of 50 Nm to the inner ring, the stress distribution cloud is shown in Fig. 3. It can be seen that the stress at root of inner ring is maximal, which is 71.364MPa. The stress value is lower than the ultimate strength of the aluminum alloy, so it meets the requirements for use.

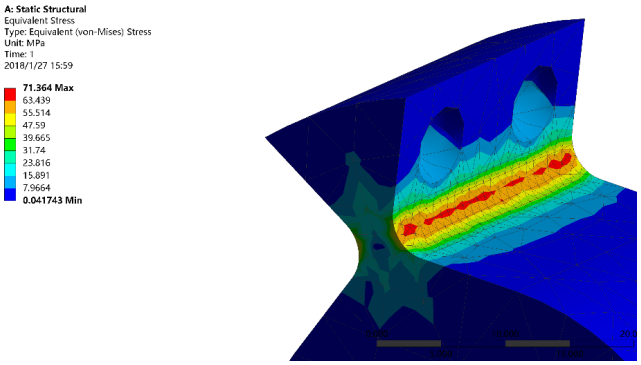

Fig. 3 The stress distribution cloud of the inner ring.

III. The Design Of SEA

In order to obtain a compact and lightweight architecture, a SEA with double-layer parallel spring was designed. The SEA joint mainly includes a brushless DC motor (EC 60 flat, Maxon Motor, Switzerland), harmonic reducer (LHD 17-80, LEADERDRIVE, China), elastic unit, magnetic encoder (ring: MRA039BC020DSE00, readhead: MB039SCB18BEDA00, Renishaw, England), base link and output link. The 3D model of the SEA joint is shown in Fig. 4. The SEA can be directly attached to the LLE knee joint.

The motor is connected to the wave generator of harmonic reducer by key. In the harmonic reducer, the rigid gear is fixed to the reducer connector and the soft gear transfer rotation to the output shaft. The output shaft and the inner ring of the elastic unit are connected by an output shaft connector. The outer ring of the elastic unit and output link connector are connected by a plate connector. Finally, the inner ring of the elastic unit rotates to drive the outer ring and transmit the rotation to the output link.

The bearing transmits the force to the output link, ensuring that the elastic unit is only subjected to torque and is not subject to radial forces. The function of the base link connector is to place the base link and the output link in the same plane, which increases the wearing comfort.

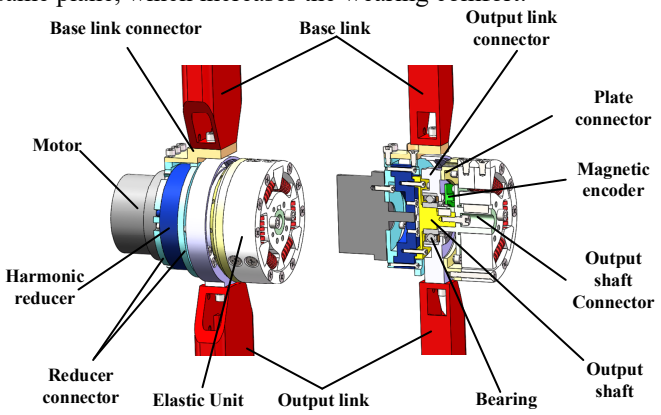

Fig. 4 3D model of the SEA joint

The motor and harmonic reducer are selected according to the kinematic characteristics of the human knee. The maximum torque of the human knee is about 40Nm, and its maximum angular velocity is ±50rpm. The maximum torque and maximum velocity of the SEA joint are respectively 54Nm and 75rpm, which can fulfill the requirements. The joint has two encoders, one of which is an encoder embedded in the motor and the other is the magnetic encoder. The encoder embedded in the motor is used to measure the angle of the output shaft. The magnetic encoder is used to measure the rotation angle of the output link relative to the output shaft (i.e., the elastic deformation angle). Furthermore, the angle of the output link can be obtained by subtracting the deformation angle from the output shaft angle. Therefore, precise position control of the output link can be achieved.

The deformation angle measured by the magnetic encoder can be used to calculate the output torque as shown in the following equation,

$$T_d = k \times \theta_d \quad (6)$$

where T_d is the output torque, θ_d is the deformation angle, and k is stiffness of the elastic unit. Therefore, it can be used for torque feedback, and precise position control can be achieved with impedance control strategy.

The resolution of the magnetic encoder is 18 bits. Therefore, the resolution of the output torque can be obtained as follows,

$$R_T = k \times \frac{2\pi}{2^{18}} = 372 \times \frac{2\pi}{2^{18}} = 0.0089\text{Nm} \quad (7)$$

where R_T is the output torque resolution, k is stiffness of the elastic unit. It can be seen that the output torque resolution can meet the requirement.

Fig. 5 shows the final assembly SEA joint. The total weight of the joint is 2.34kg. The diameter of the inner ring of the elastic unit is 20 mm. The diameter of the outer ring of the

elastic unit is 94 mm. The thickness of the elastic unit is 26 mm. All of these parameters meet the design requirements.

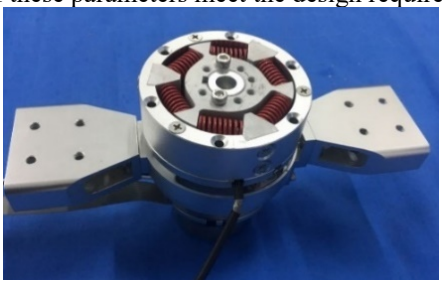

Fig. 5 The final assembly SEA joint.

IV. Modeling And Control

A. Modeling

The transfer function of the SEA can be obtained through the dynamic model. The model of the SEA is shown in Figure 6. In order to obtain the transfer function between the motor torque and the load torque, it is assumed that the load is fixed, that is θ_L=0. Regarding Fig. 6, the input torque (T_{in}) of the reducer can be expressed by,

$$T_{in}(s) = T_M(s) - J_M\theta_M(s)s^2 - B_M\theta_M(s)s \tag{8}$$

where θ_M is the motor rotation angle, T_M is the motor output torque, J_M is the inertia coefficient of the motor, and B_M is the damping coefficient of the motor. The output torque (T_{out}) of the reducer can be expressed as follows,

$$T_{out}(s) = \left(J_R + J_S\right)\theta_R(s)s^2 + B_R\theta_R(s)s + T_L(s) \tag{9}$$

where θ_R is the reducer rotation angle, T_L is the torque applied to the load, J_R is the inertia coefficient of the reducer, J_S is the inertia coefficient of the elastic unit, and B_R is the damping coefficient of the reducer.

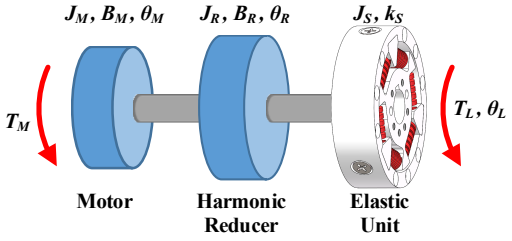

Fig. 6 The model of SEA.

Since the torque of the motor is amplified by the harmonic reducer by N times (N is the reduction ratio of the reducer), the following equation can be obtained:

$$T_{out}(s) = NT_{in}(s) \tag{10}$$

and

$$\theta_M(s) = N\theta_R(s) \tag{11}$$

Substituting Eq. (8) and Eq. (9) into Eq. (10), and Eq. (11) into the resulting equation, one obtains

$$\begin{aligned} NT_M(s) = &\left(N^2J_M + J_R + J_S\right)\theta_R(s)s^2 + \\ &\left(N^2B_m + B_R\right)\theta_R(s)s + T_L(s) \end{aligned} \tag{12}$$

Eq. (12) can be simplified as:

$$NT_M(s) = J_{eq}\theta_R(s)s^2 + B_{eq}\theta_R(s)s + T_L(s) \tag{13}$$

where $J_{eq}=N^2J_M + J_R + J_S$ is the equivalent rotational inertia and $B_{eq}=N^2B_M + B_R$ is the equivalent damping coefficient. The $\theta_R(s)$ can be rewritten as:

$$\theta_R(s) = T_L(s)/k_S + \theta_L(s) \tag{14}$$

where k_S is the stiffness of elastic unit. To overcome some undesired effects by motor internal disturbance, the motor is treated as a velocity source. Considering that the required current is equal to the actual current, the motor torque can be calculated as,

$$T_M(s) = k_t\left[K_{PV}\left(\omega_m^d(s) - \omega_m(s)\right) + K_{IV}\frac{\left(\omega_m^d(s) - \omega_m(s)\right)}{s}\right] \tag{15}$$

where $\omega^d{}_m(s)$ is the desired velocity, $\omega_m(s)=N\theta_R(s)s$ is the actual velocity, k_t is the motor torque constant, K_{PV} is the proportion gains, K_{IV} is the integration gains.

Substituting Eq. (15) into Eq. (13), and Eq. (14) into resulting equation, one obtains,

$$\begin{aligned} T_L(s) = &\frac{\left(\frac{Nk_sk_tK_{PV}}{J_{eq}}\right)s + \left(\frac{Nk_sk_tK_{IV}}{J_{eq}}\right)}{s^3 + \left(\frac{B_{eq} + N^2k_tK_{PV}}{J_{eq}}\right)s^2 + \left(\frac{k_s + N^2k_tK_{IV}}{J_{eq}}\right)s}\omega_M^d(s) - \\ &\frac{k_ss^3 + \left(\frac{B_{eq}k_s + N^2k_sk_tK_{PV}}{J_{eq}}\right)s^2 + \left(\frac{N^2k_sk_tK_{IV}}{J_{eq}}\right)s}{s^3 + \left(\frac{B_{eq} + N^2k_tK_{PV}}{J_{eq}}\right)s^2 + \left(\frac{k_s + N^2k_tk_{IV}}{J_{eq}}\right)s}\theta_L(s) \end{aligned} \tag{16}$$

Considering that the load is fixed ($\theta_L(s)$=0), the transfer function between the load torque and the motor velocity can be expressed as follows,

$$\begin{aligned} G(s) &= \frac{T_L(s)}{\omega^d{}_M(s)} \\ &= \frac{\left(\frac{Nk_sk_tk_p}{J_{eq}}\right)s + \left(\frac{Nk_sk_tk_i}{J_{eq}}\right)}{s^3 + \left(\frac{B_{eq} + k_tk_pN^2}{J_{eq}}\right)s^2 + \left(\frac{k_s + k_tk_iN^2}{J_{eq}}\right)s} \end{aligned} \tag{17}$$

B. Control

The SEA joints in this paper use impedance control strategies to improve the comfort of human-machine interaction. The block diagram of the control scheme is shown in Figure 7.

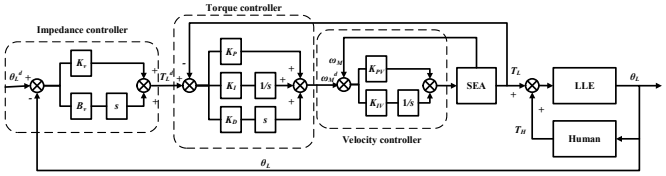

Fig. 7 Control scheme.

The outer loop of the controller is impedance control, and the inner loop of the controller is velocity control. The PID torque control is used to generate the desired velocity, which is used as the input of the PI velocity controller. The impedance control can calculate the desired torque according

to the desired angle and the actual feedback angle, which can be expressed by the following formula:

$$T_L^d = K_v\left(\theta_L^d - \theta_L\right) + B_v\left(\dot{\theta}_L^d - \dot{\theta}_L\right) \quad (18)$$

where K_v is the virtual stiffness, and B_v is the virtual damping.

V. Experimental Tests

A. Elastic unit calibration experiment

In order to obtain the real elastic unit stiffness, the calibration experiments were carried out. The experimental platform is shown in Figure 8. The inner ring of the elastic unit is fixed, and the outer ring of the elastic unit is connected to a rod. Different torque values are obtained by changing the weight and the length of the arm, and the rotation angles are measured by the encoder. The power supply is used to supply power to the encoder. The encoder communicates with the PC through the CAN-USB adapter. The weight can be hung on both sides of the rod. That is, a positive torque is generated on one side and a negative torque on the other side.

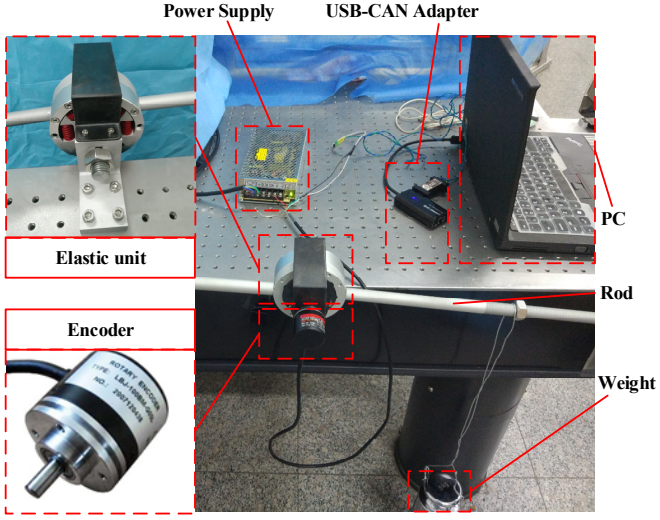

Fig. 8 Elastic unit stiffness calibration experiment platform.

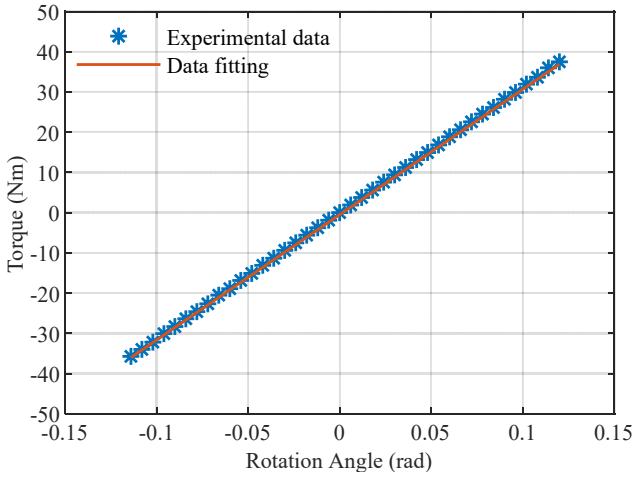

Fig. 9 Characterization of the elastic unit.

Fig. 9 shows the relationship between the torque and rotation angle of the elastic unit. The fitting curve can be obtained as follows,

$$T_E = 311.6 \times \theta_E - 0.5079 \quad (19)$$

where T_E is the torque and θ_E is the rotation angle. Linear regression has a correlation coefficient $R^2 = 0.981$. It can be seen that the linearity of the elastic unit is good. The stiffness of elastic unit is approximately 312Nm/rad. The experimental stiffness is around 16% lower than the predicted one. This may be due to the fact that the stiffness of the rectangular spring is less than the theoretical value.

B. Impedance control for the SEA in LLE

The SEA is designed for our previously developed LLE [15]. The knee joint of LLE adopts SEA. The Elmo driver (type: G-SOLTWI 10/100SE) is chosen to drive the motor. The ARM-Cortex-A9 board as the main controller for collecting information and sending commands. CANopen protocol is used between the main controller board and the driver, the transmission rate can reach 1 Mbit/s.

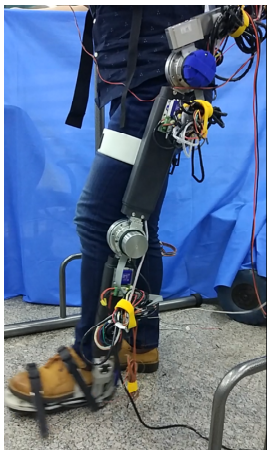

Fig. 10. The LLE with SEA

To test the impedance control performance, a volunteer wears the exoskeleton to track the knee reference trajectory, which is shown in Fig. 10. The LLE knee joint is commanded to track trajectories with low impedance and high impedance. For the proposed control, the high impedance parameters are selected as K_v = 120 Nm/rad, B_v = 15 Nms/rad and the low impedance parameters are selected as K_v = 30 Nm/rad, B_v = 8 Nms/rad. Three frequency reference trajectories were designed to evaluate the tracking performance of the proposed control method. These three reference trajectories are designed as 15+15sin(πt-π/2), 15+15sin(2πt-π/2) and 15+15sin(5πt-π/2) degrees.

Figure 11 shows a comparative study result of the tracking performance of three frequency motions between high impedance and low impedance. Generally, the impedance control exhibits superior tracking performance in following motion at several frequencies. This illustrates that the SEA has a wider operating bandwidth under the impedance control. It can be seen that the tracking trajectory error becomes larger as the frequency increases. Moreover, the tracking error is small at high impedance state and large at low impedance state. Therefore, the impedance coefficient can be determined according to the use situation. That is, high impedance parameters are used when high tracking accuracy is required, and low impedance parameters are used when high comfort is required.

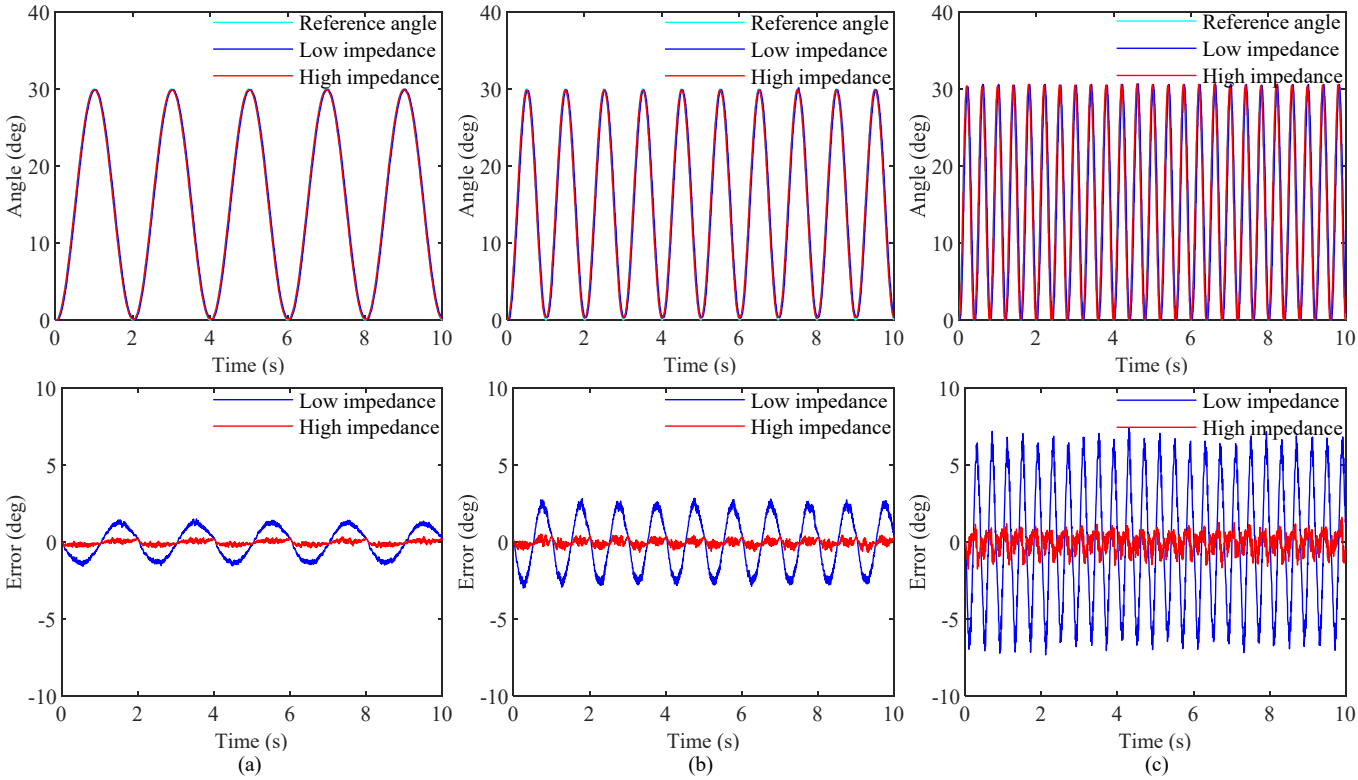

Fig. 11 Position tracking performance at several frequencies. (a) 15+15sin(πt-π/2), (b) 15+15sin(2πt-π/2) (a) 15+15sin(5πt-π/2)

VI. Conclusion

This paper presents a novel SEA for LLE that uses double-layered parallel springs. Verify that the characteristics of the SEA through finite element analysis and calibration experiments, and the results showed that they met the design requirements. Further, the impedance controller was designed for the SEA joint. Preliminary experimental results show that impedance control shows a wider operating bandwidth and also shows the relationship between tracking performance and impedance parameters. In the future, more types of experiments will be conducted, such as walking and going up and down stairs.

Acknowledgment

This work was supported by the Pre-research project in the manned space field, Project Number 020202, China.

References

[1] T. Yan, M. Cempini, C. M. Oddo, and N. Vitiello, “Review of assistive strategies in powered lower-limb orthoses and exoskeletons,” Robotics and Autonomous Systems, vol. 64, pp. 120-136, Feb. 2015.

[2] L. Yi, Z. Du, C. Chen, W. Wang, H. Long, X. Mao, G. Xu, G. Zhao, X. Li, and D. Wei, “Development and Analysis of an Electrically Actuated Lower Extremity Assistive Exoskeleton,” Journal of Bionic Engineering, vol. 14, no. 2, pp. 272-283, 2017.

[3] A. Calanca, R. Muradore, and P. Fiorini, “Impedance control of series elastic actuators: Passivity and acceleration-based control,” Mechatronics, vol. 47, pp. 37-48, 2017.

[4] L. Xiang, Y. Pan, C. Gong and H. Yu, “Adaptive Human–Robot Interaction Control for Robots Driven by Series Elastic Actuators,” IEEE T. Robot., vol. 33, no. 1, pp. 169-182, 2017.

[5] C. Lagoda, A. C. Schouten, A. H. A. Stienen, E. E. G. Hekman and H. V. D. Kooij. “Design of an electric Series Elastic Actuated Joint for robotic gait rehabilitation training,” Proceedings of the 2010 3rd IEEE RAS & EMBS, pp. 21-26, 2010.

[6] G. Carpino, D. Accoto, F. Sergi, N.L. Tagliamonte and E. Guglielmelli, “A novel compact torsional spring for series elastic actuators for assistive wearable robots,” J. Mech. Design, vol. 134, no. 12, pp. 121002, 2012.

[7] W.M. Dos Santos, G.A. Caurin and A.A. Siqueira, “Design and control of an active knee orthosis driven by a rotary series elastic actuator,” Control Eng. Pract., vol. 58, pp. 307-318, 2017.

[8] Y. Long, Z. Du, C. Chen, W. Wang and W. Dong, “Development of a lower extremity wearable exoskeleton with double compact elastic module: preliminary experiments,” Mechanical Sciences, vol. 8, no. 2, pp. 249-258, 2017.

[9] N. C. Karavas, N. G. Tsagarakis and D. G. Caldwell. “Design, modeling and control of a series elastic actuator for an assistive knee exoskeleton,” In 2012 4th IEEE RAS & EMBS Int. Conf. on Biomedical Robotics and Biomechatronics. pp. 1813-1819. 2012.

[10] M. Cestari, D. Sanz-Merodio and E. Garcia, "Preliminary assessment of a compliant gait exoskeleton," Soft robotics, vol. 4, no. 2, pp. 135-146, 2017.

[11] Y. Zhu, J. Yang, H. Jin, X. Zang, and J. Zhao. “Design and Evaluation of a Parallel-Series Elastic Actuator for Lower Limb Exoskeletons,” In 2014 IEEE Int. Conf. on Robotics and Automation, pp. 1335-1340. 2014.

[12] W.M. Dos Santos and A.A. Siqueira, “Impedance control of a rotary series elastic actuator for knee rehabilitation,” IFAC Proceedings Volumes, vol. 47, no. 3, pp. 4801-4806, 2014.

[13] K. Kong, J. Bae and M. Tomizuka, “A compact rotary series elastic actuator for human assistive systems,” IEEE/ASME transactions on mechatronics, vol. 17, no. 2, pp. 288-297, 2011.

[14] D.A. Winter, “Biomechanics and motor control of human movement,” John Wiley & Sons, 2009.

[15] C. Chen, Z. Du, L. He, J. Wang, D. Wu and W. Dong, “Active Disturbance Rejection With Fast Terminal Sliding Mode Control for a Lower Limb Exoskeleton in Swing Phase,” IEEE Access, vol. 7, pp. 72343-72357, 2019.